Geophysical Journal (1988) **94**, 377–386

South American–Antarctic plate motion over the past 50 Myr, and the evolution of the South American–Antarctic ridge

Peter F. Barker
British Antarctic Survey, High Cross, Madingley Road, Cambridge CB3 OET, UK

Lawrence A. Lawver
Institute for Geophysics, University of Texas at Austin, 8701 *North Mopac Blvd., Austin, Texas* 78759-8345, *USA*

Accepted 1988 February 18. Received 1988 February 18; in original form 1986 December 31

SUMMARY

Magnetic and bathymetric data from the South American–Antarctic plate boundary east of the South Sandwich trench have been interpreted to produce ocean floor ages, spreading rates and directions. SAM–ANT motion over the past 50 Myr has been slow (10–15 mm yr^{-1} half rates). About 20 Ma the spreading direction changed from 120°–300° to the present E–W. These results have been combined with similar data from the South Atlantic and Southwest Indian Oceans to calculate six poles and rates of SAM–ANT motion covering the past 50 Myr. The change at 20 Ma appears to have originated the long-offset Bullard and South Sandwich fracture zones. The change may have been facilitated, or even triggered, by ridge crest–trench collision along the South Scotia Ridge, east of the South Orkney Islands. This event however, could not alone have caused a stable change. It is concluded that the global balance of forces may for long periods be imperfectly reflected in plate motions, because of the constraining effects of long fracture zone offsets on the directions of plate motion, and that the 'causes' of abrupt changes in direction may precede them by several million years.

Key words: Antarctic, South Atlantic, plate motion, plate boundaries, fracture zones, driving forces

INTRODUCTION

The Cenozoic history of relative motion of the South American and Antarctic plates is of great interest in many fields of earth science. Yet, for a range of reasons, that history is poorly known. We report here an attempt to obtain a more precise and detailed estimate than has been available hitherto.

Existing calculations of South American–Antarctic motion are of two kinds. In the first (e.g. Chase 1978; Minster & Jordan 1978), earthquake first motions, transform faults and 'instantaneous' spreading rates are used to solve the *N*-plate problem for present plate motions. A typical result (Minster & Jordan 1978) shows South America to be rotating anticlockwise at *ca.* 0.30° Myr^{-1} about a pole at 88°S 105°W. Estimates of this kind are generally precise, but cannot be extrapolated far back in time. Estimates of the second kind, using fracture zones and magnetic anomalies to compute finite rotation poles and angles, have been concerned mainly with models of Gondwanaland and its break-up. They suffer two disadvantages from our point of view: the time steps are coarse (*ca.* 20 Myr—Norton & Sclater 1979, for example) and the data sets used have not included any from the South American–Antarctic plate boundary itself.

The boundary between the South American and Antarctic plates (Fig. 1) can be divided into three parts, two of which are incapable of providing data which will constrain past plate motions. In the far west, the plate boundary lies at the Chile trench. Between the triple junction at 46°S and the western Straits of Magellan at 52°S, Antarctic oceanic lithosphere is being subducted eastward beneath South America at the slow rate of 20–24 mm yr^{-1} (Minster & Jordan 1978). This slow subduction province was created about 15 Ma when the Pacific–Nazca spreading centre was subducted, and currently is extending northward (Herron, Cande & Hall 1981; Cande, Herron & Hall 1982; Cande & Leslie 1986). In a second, central province, between the western Straits of Magellan and the southern South Sandwich trench, a simple South American–Antarctic plate boundary does not exist because of the intervention of a number of small plates. This complication has evolved over the past 40 Myr by the eastward migration of a subduction zone similar to that of the present South Sandwich trench, and the growth behind it of the Scotia Sea during a number of short, overlapping episodes of back-arc extension (Barker & Hill 1981; Barker, Barber & King 1984). The third, eastern part of the South American–Antarctic plate boundary (boxed in Fig. 1), is the only one whose Cenozoic history can be mapped easily, and used to

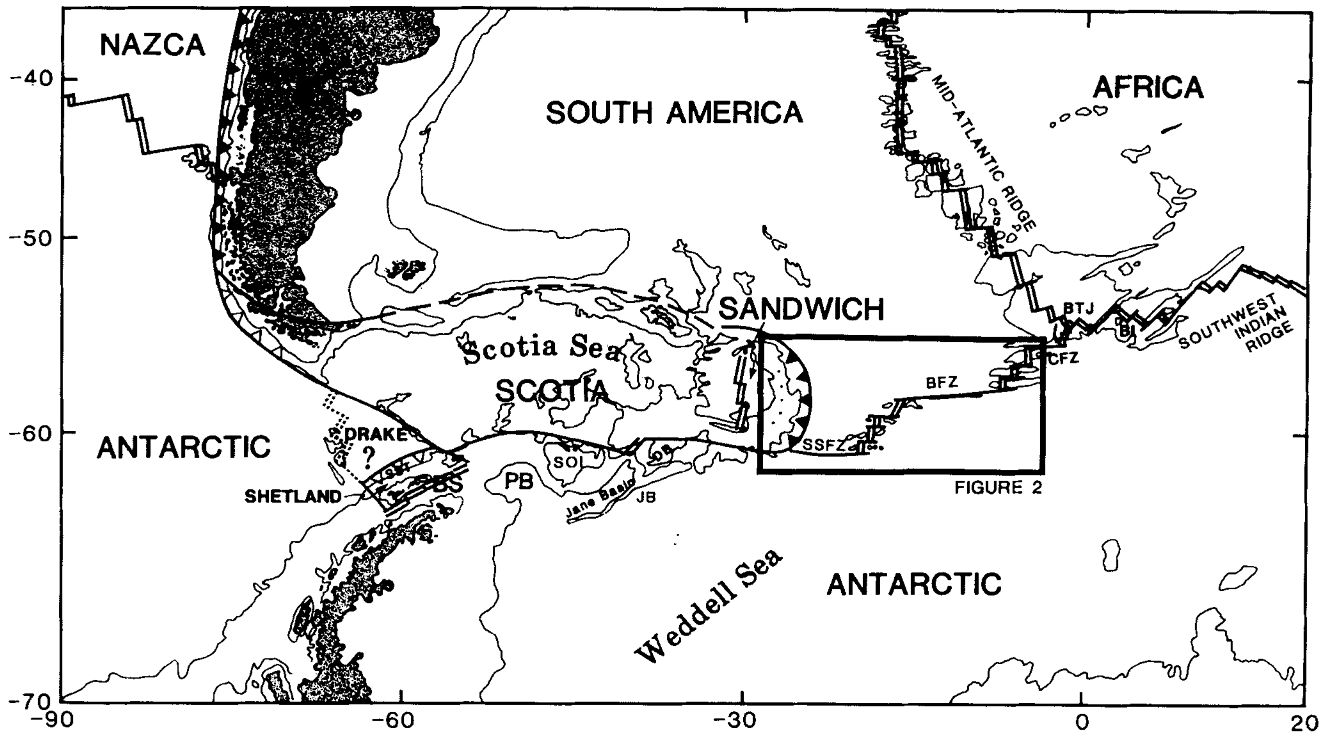

Figure 1. Generalized diagram showing the location of the South American–Antarctic Ridge, Southwest Indian Ridge, Mid-Atlantic Ridge, Scotia Sea and Weddell Sea. Spreading centres are indicated by double line segments, active faults shown by single lines and trenches or presumed zones of underthrusting shown by toothed line. The 200 m and 3000 m contours are shown in light lines. CFZ: Conrad Fracture Zone; BFZ: Bullard Fracture Zone; SSFZ: South Sandwich Fracture Zone; BTJ: Bouvet Triple Junction; BI: Bouvet Island; JB: Jane Bank; SOI: South Orkney Islands; DB: Discovery Bank; PB: Powell Basin; BS: Bransfield Strait; SST: South Shetland Trench.

constrain models of major plate motion. This province, the South American–Antarctic Ridge (SAAR), extends from the southern South Sandwich trench to the Bouvet triple junction. It is extensional, with short N–S ridge crest sections separating several short and two long transform faults oriented slightly south of west. We examine it in detail here.

The nature of the SAAR was first inferred from earthquake epicentre distributions (Barker 1970; Forsyth 1975) and first motion studies. Present-day plate motion has been calculated from both local (Forsyth 1975; Sclater *et al.* 1976) and global data sets (Chase 1978; Minster & Jordan 1978). The local observations extended back to anomaly 3 (Sclater *et al.* 1976) and anomaly 5 (Lawver & Dick 1983) but no farther. They showed motion slightly south of west, and slow (*ca.* 20 mm yr^{-1}), in accord with the global *N*-plate solutions.

The coarse, Gondwanaland break-up models, based on South Atlantic and Indian Ocean magnetic anomalies and fracture zones (e.g. Norton & Sclater 1979; Lawver, Sclater & Meinke 1985), show South American–Antarctic motion to have been originally closer to north–south, and to have swung through NW–SE to the present W–E orientation through the Cretaceous and Cenozoic. The details of this change in orientation are poorly constrained, but fracture zone topography (Barker & Jahn 1980; Tectonic Map 1985) and magnetic anomalies (LaBrecque & Barker 1981) in the Weddell Sea provide independent corroboration. The level of description of South American–Antarctic motion provided by these models is adequate for many purposes, but not for all. For example, a precise knowledge of the positions of the bounding major plates is important to studies of Scotia Sea evolution, particularly those seeking to understand the origin of the east-migrating subduction or the development of the deep-water pathway between Pacific and Atlantic Oceans now occupied by the Antarctic Circumpolar Current (e.g. Barker & Burrell 1977). For these, the coarseness of the time steps and absence of constraints from the South American–Antarctic plate boundary itself are crucial weaknesses, which we have tried to remove.

We have compiled and interpreted all of the available marine bathymetric and magnetic data from the region between the South Sandwich trench and the Bouvet triple junction, and have also considered the regional earthquake epicentre distribution and SEASAT-derived gravity. The interpreted data have been combined with similar published data from the South Atlantic and Southwest Indian Oceans to provide a series of six total opening poles and rotation rates for South American–Antarctic motion extending back to Anomaly 21 (*ca.* 50 Myr). The results, besides being of potential value to the kinds of study mentioned, throw light on the origin of the long-offset transform faults which dominate the SAAR at present.

DATA COMPILATION AND REDUCTION

For the area boxed in Fig. 1 we have combined UK satellite-fixed magnetic and bathymetric data with tnose available from the US National Geophysical Data Centre.

These profiles had accumulated over the past 15–20 yr and many were previously unpublished. The bathymetric data on which the contoured chart (Fig. 2) is based also included some older, less well-fixed soundings from UK Admiralty ocean plotting sheets, used where they were not in conflict with more recent data. The earthquake epicentres also plotted in Fig. 2 are from the US National Earthquake Information Service.

Bathymetry

In the western part of Fig. 2 lies the South Sandwich island arc, fore-arc and trench. East of there, the bathymetry is dominated by the ridge crests, median valleys and transform faults of the South American–Antarctic plate boundary. These features are delineated also by the earthquake epicentres. The South Sandwich fore-arc shows intense earthquake activity also, but epicentres west of the trench are not shown in Fig. 2 so as to avoid masking the bathymetry.

The ridge crest sections of the SAAR are oriented approximately N–S and the transform faults strike slightly north of east. The transform offsets are short (less than 100 km) with the exceptions of the 200 km-long Conrad fracture zone in the northeast, and the Bullard fracture zone near 58°S (Lawver & Dick 1983) and South Sandwich fracture zone near 61°S, both of which exceed 400 km in length. The topographic relief at the plate boundary is extreme; median valleys are typically 1.5–2 km deeper than adjacent ridges, and at several sites on the Bullard and South Sandwich fracture zones the relief exceeds 3 km. The mean ridge crest elevation in the region between 15° and 20°W is close to the 2.5 km average for the world's oceans calculated by Parsons & Sclater (1977). In the east, closer to the Bouvet triple junction, the ridge crest is shallower. Away from the ridge crest, the sea-floor deepens in general accord with a steadily increasing ocean-floor age, except at the elevated outer swell of the South Sandwich trench between about 24° and 21°W. It is worth noting that in a few places (for example northwest of the Bullard fracture zone and southeast of the South Sandwich fracture zone) the gross fabric of the bathymetry appears to rotate from west–east around towards northwest–southeast.

Magnetic anomalies

Figure 3 shows magnetic anomalies plotted along ship tracks after removal of the IGRF (IAGA, 1981). Positive anomalies are to the north and west. Selected anomalies are identified by comparison with synthetic anomalies generated using the time scale of LaBrecque, Kent & Cande (1977), a depth to top coincident with the subsidence curve of Parsons & Sclater (1977), and other generally accepted parameters. Fracture zone locations are based mainly on bathymetric features, not all of which are sufficiently large to show prominently in Fig. 2.

Magnetic anomalies on the northernmost track in Fig. 3 were generated at a half spreading rate of about 20 mm per year. Comparison with data from near the Falkland–Agulhas fracture zone (Barker 1979) shows that these anomalies formed at the mid-Atlantic Ridge. A fracture zone, cutting the profile near 14°W, causes the repeat of anomaly 13 and shows an offset of 150 km. Anomalies 13–21 on the next lines south (near 56.3°S between 12 and 16°W), though less well-formed, show similar fast spreading rates and were assumed initially also to have formed at the mid-Atlantic Ridge. We shall show later that this may not have been the case.

All of the other identified anomalies in Fig. 3 were formed at the SAAR. Fig. 4 shows a selection of magnetic profiles compared with a synthetic anomaly profile generated using half spreading rates of between 9.5 and 14 mm yr^{-1}. The quality of the correspondence between observed and synthetic anomalies across the entire region is variable. However, there are sufficient sections of the profile where the correspondence is good, to validate the general interpretation. For example, many additional profiles now confirm the correlations from the ridge crest to anomaly 5 proposed by Lawver & Dick (1983). These correlations can be extended beyond anomaly 6 on profiles D, F and G in Fig. 4, with anomaly 5b being particularly distinctive throughout the region. The correlation from anomaly 6 to anomaly 8 is reasonable on profiles B and F, and the section from there back to anomalies 13 and 21 is confirmed by the combination of profiles D, E and F. The fracture zone which cuts profiles D, E and F in Fig. 4, and the eastward extension of the South Sandwich FZ which parallels it to the south in Figs. 2 and 3 are important. They suggest a change in the direction of spreading at about the time of anomaly 6 (*ca.* 20 Ma). The other indication of a NW–SE ocean floor fabric (in Fig. 2) has already been mentioned. The fracture zone which intersects the South Sandwich trench near 56°S has a similar orientation and is orthogonal to adjacent (though undated) magnetic anomalies. These are all indications of an earlier spreading direction different from the present E–W. Additional evidence comes from the gravity anomaly map derived from SEASAT radar altimeter measurements (Haxby 1985), part of which forms Fig. 5. SEASAT transmitted for only three months, during the Antarctic Winter and early Spring when pack ice cover was farthest north. In this region the pack ice edge lay north of 60°S. To the south, the poor reflectivity of the ice greatly reduced the quality of the altimeter data, so that only the larger ocean floor features are visible. Nevertheless, some indication of a curvature of the ocean floor fabric towards NW–SE, from W–E near the present plate boundary, may be seen.

We will return later to the topic of changes in spreading direction. It is important to note now, however, the uncertainty which such changes impose on the interpretation of a magnetic anomaly map based on the rather uneven and sparse distribution of ship tracks available here. It is known from other, better-mapped areas that a change in spreading direction can involve the production of fan-shaped anomalies, asymmetric spreading, the abandonment and creation of transform faults, and small ridge jumps. To these effects we may owe the rather poor quality of some of the anomaly correlations. Also, they will make our estimates of spreading rate at best only approximate. Thus, the half spreading rates appear to lie in the range 9–12 mm yr^{-1} (Fig. 4), except for the period between about 42 and 27 Ma, when faster rates (up to 15 mm yr^{-1}) seem necessary. We cannot insist on more precise values than these at present. In particular, the model values are not in conflict with the

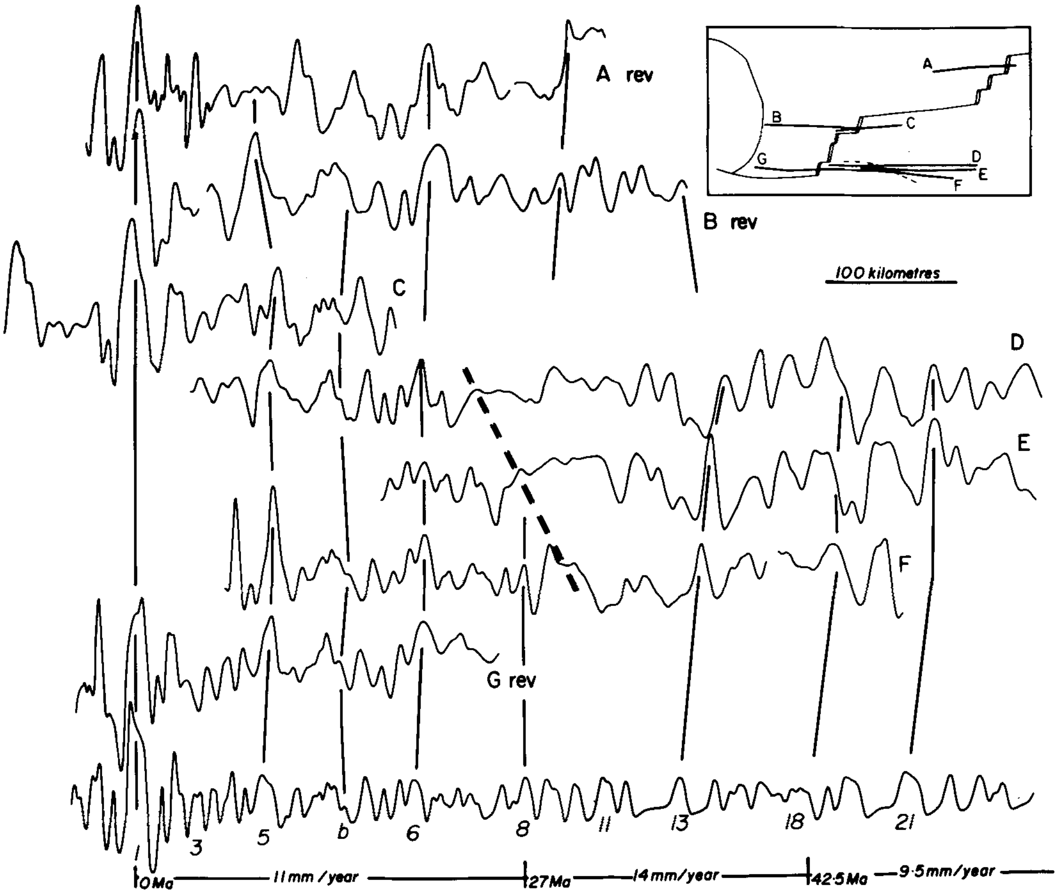

Figure 4. Magnetic anomalies along selected tracks (located on inset) compared with synthetic profile based on LaBrecque *et al.* (1977) timescale. Fracture zone cutting some tracks is shown dashed. Observed profiles are resolved along 095°, so older spreading rates (before 20 Myr) may be *ca.* 10 per cent higher than shown.

9 mm yr^{-1} half-rate for the last 9 Myr calculated by Lawver & Dick (1983).

Besides the SAM–ANT plate motion, SAM–AFR motion has generated some of the fracture zone topography revealed in Fig. 5, including a fracture zone which offsets magnetic anomaly 13, already discussed. The other magnetic anomalies appearing to have been produced at a fast spreading rate, located near 56.5°S, 16°W, lie within that part of Fig. 5 which shows the older 120–300° SAM–ANT fabric. The apparent fast spreading is thus an artefact of an oblique crossing and perhaps of repetition across small-offset fracture zones. The magnetic bight which forms the southwestern trace of the Bouvet triple junction passes through the region of Figs 2 and 3: the behaviour of the modern triple junction is complicated, so that isolated magnetic profiles should be interpreted with care.

Before considering other plate boundaries, we would mention the cluster of earthquake epicentres near 59.4°S, 20–22°W (Fig. 2), for one of which Farmer, Fujita & Stein (1982) computed a dextral E–W strike-slip first motion. This sense suggests faster subduction of the younger southern part of the sinking South American ocean floor, incompatibly with the expected age–buoyancy relation and Benioff Zone earthquake data (Isacks & Molnar 1971; Forsyth 1975). While the independent motion of small plates being subducted is well documented (Menard 1978), there is no obvious difference between recent spreading rates at the southwestern and northeastern parts of the SAAR, and an intraplate origin for this particular earthquake seems equally likely.

SOUTH AMERICAN–AFRICAN–ANTARCTIC MOTION

The identified magnetic anomalies and fracture zones provide constraints on South American–Antarctic plate motion more directly than any data previously available. They come from only a small area, however, and would not alone give precise estimates of poles of rotation. We have chosen rather to combine them with existing data of similar kind from the South Atlantic and Indian Oceans, to constrain together the motions of the South American, Antarctic and African plates. We had available two methods of extracting formal Euler poles and rotation rates, the Evans and Sutherland 3-D computer graphics system (Scotese, Gahagan & Larson 1988) and a separate three-plate iterative fitting program (Tapscott 1979). These methods are complementary, compensating to a large extent for each other's weaknesses.

The Evans and Sutherland system provides fast, precise

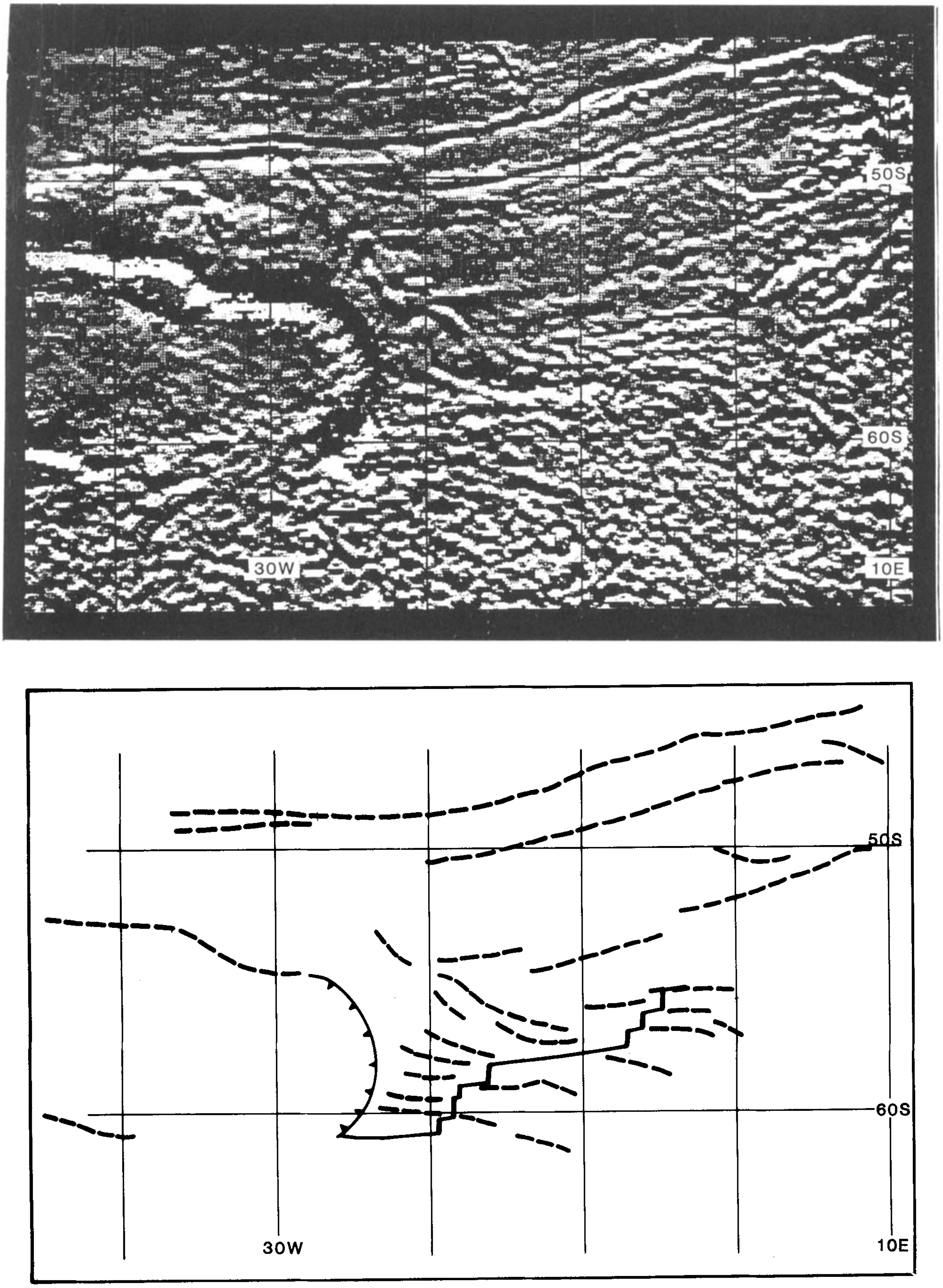

Figure 5. Portion of Seasat gravity map (Haxley 1985), with lineations extracted which are probably fracture zone traces.

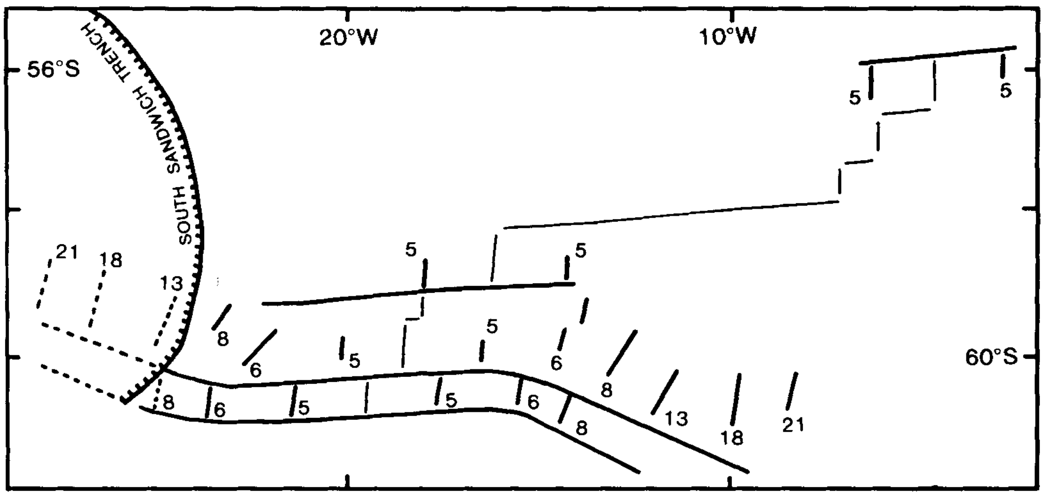

Figure 6. Subset of fracture zone and anomaly data from Figs 2 and 3 in 3-plate fitting exercise which produced poles and rates quoted in Table 1. Note that only short sections of fracture zones were used for each anomaly fit, to avoid spurious coincidence. Anomalies located by extrapolation, assuming symmetric spreading, are shown dashed. The position of the present SAM–ANT boundary is shown faint.

and documented 3-D rotation and display on any scale of a number of large, coherent data sets. At UT Austin where such a system is operated under the Paleo-Oceanographic Mapping Project (POMP) these data sets are lithospheric plates (coastlines, magnetic anomalies, fracture zones etcetera). With help from colleagues we digitised published data from the South Atlantic (Ladd 1974; Barker 1979; Rabinowitz & LaBrecque 1979) and southwest Indian Ocean (Bergh & Norton 1976; Sclater *et al.* 1976; LaBrecque & Hayes 1979; Norton & Sclater 1979; Goslin, Recq & Schlich 1980; Schlich 1983; Fisher & Sclater 1983; Patriat 1983), in addition to the newly derived SAAR data. Reconstructions were attempted for six times, at 7–10 Myr intervals through the last 50 Myr, for which a reasonable number of anomaly identifications existed on all three plate boundaries.

The method has several advantages, not least of which are its speed and flexibility once the data are accessible. Also, it permits reconstructions of a kind, when data are available from only one side of the spreading centre (as on the SAAR, where the older anomalies on the South American plate have been subducted—Fig. 3), by rotating anomalies back to the present ridge crest. However, the difficulties of trying manually to obtain a precise fit at more than one plate boundary simultaneously make the operator unconvinced that the fit achieved is optimal. This is particularly the case when, as here, the data sets are of uneven quality and distribution. The uncertainties in the SAAR data have already been mentioned. Also, however, the South Atlantic data of Ladd (1974), in the form available, comprise real magnetic anomaly identifications but *synthetic* fracture zones, no doubt close to the observed data but not necessarily coincident. In addition, the southwest Indian Ocean is logistically remote, so that few magnetic profiles exist. Also, it has opened only slowly and in a direction oblique to the overall orientation of the plate boundary, which has produced poorly formed anomalies, making identification prone to error. We checked the actual data wherever possible, but our re-interpretations are not necessarily better than the originals.

In an attempt to optimise the reconstructions, we used an automatic iterative fitting program, an extension to three plates by Tapscott (1979) of the two-plate method of Hellinger (1981). The data set (Fig. 6) was a refined subset of that digitised for use with the Evans and Sutherland system, divided into numbers of corresponding segments on each flank of a plate boundary and with an error parameter (in km) attached to each observation to weight its contribution to the fit. Lack of data on one flank of a fracture zone or ridge crest segment generally precluded the use of any data from that segment, since it was not simple to combine full rotations (anomaly to anomaly) and half rotations (to the ridge crest) in one computation. In the case of the SAAR data however, some consideration was allowed of the older anomalies recently subducted at the South Sandwich trench, by extrapolating back from the oldest surviving anomaly at the half-rate observed on the opposing flank, attaching a suitably enlarged error estimate. In fact, this method is more accurate than rotation to the ridge crest, since the effects of any asymmetric spreading more recently than the period covered by the extrapolation are eliminated.

The initial estimates inserted into these automatic iterative calculations were those produced by the earlier work using the Evans and Sutherland system. The first series of iterations appeared successful, reducing the measure of misfit (in 'error estimate' units) by between 15 and 70 per cent for the six times (anomalies) selected. Furthermore, the reconstructions appeared reasonable when re-examined using the Evans and Sutherland display. At a later stage, Cande made available to us the results of a detailed re-assessment of South Atlantic opening (S. C. Cande private communication), which used a more extensive marine geophysical data set than that available to Ladd (1974). A recomputation which held SAM–AFR motion fixed, using these new data, further improved the three-plate fit. In this final recomputation, the summed weights of all of the matched segments amounted to approximately one-third Southwest Indian Ridge and two-thirds SAAR. It is important to note, however, that the

Table 1. Calculated South American–African–Antarctic motion through the past 50 myr

A	B	Stage	Lat.	Long.	Angle	Period (Myr)	Anom.
3	2	1	56.43	−37.81	−3.67	9.74–0	A05(o)
3	2	2	55.28	−35.45	−7.45	20.07–0	A06(o)
3	2	3	55.61	−34.00	−10.37	27.54–0	A08(o)
3	2	4	57.09	−33.78	−13.43	35.26–0	A13(y)
3	2	5	57.14	−32.31	−16.57	42.88–0	A18(o)
3	2	6	57.66	−30.96	−19.59	50.67–0	A21(o)
3	1	1	79.65	−29.87	−2.91		
3	1	2	76.43	−26.81	−5.87		
3	1	3	76.01	−6.26	−7.70		
3	1	4	77.21	2.08	−9.97		
3	1	5	74.30	11.84	−12.23		
3	1	6	76.65	20.57	−15.11		
2	1	1	7.42	−39.15	1.53		
2	1	2	8.11	−36.80	2.92		
2	1	3	13.72	−42.06	4.43		
2	1	4	14.63	−42.31	5.86		
2	1	5	15.72	−45.83	7.31		
2	1	6	11.46	−41.20	8.55		

A is fixed plate; B moving plate. 3 is SAM; 2 is AFR; 1 is ANT. 3–2 data from S. C. Cande (personal communication 1986), interpolated to anomalies listed. Ages from LaBrecque *et al.* (1977). Convention sets rotation angle positive if motion seen from above the stated pole is clockwise.

data sets from the SAAR and the Southwest Indian Ridge remain very uncertain, and that the quantification of this uncertainty, for use (inverted) as a weighting factor in the iterative fitting computation, is itself subjective.

The final rotation parameters are set out in Table 1.

DISCUSSION

In Fig. 7 we show synthetic fracture zones (or flow lines) of South American–Antarctic motion over the past 50 Myr, produced using stage poles and rates derived from the rotation parameters in Table 1. The starting point for each flow line is an intersection of a present-day ridge crest with a transform fault. To aid understanding, a 'synthetic magnetic anomaly' of the same length and orientation as the present ridge crest is drawn on the appropriate side of each stage position on the flow line, and alongside a few flow lines are noted the calculated spreading rates for each interval, for comparison with Fig. 4.

The most prominent feature of Fig. 7 is the change in spreading direction at anomaly 6 time (*ca.* 20 Myr). This mirrors the change in the observed data at about this time, to be seen in Fig. 4. The change illustrated in Fig. 7 gains validity, however, from being the result of a least-squares fit of both the SAAR data and similar data from considerable lengths of the South Atlantic and Indian Oceans. Indeed, considering that the fit for each of the six anomalies chosen was virtually completely independent of the others, the straightness of the flow lines (the anomaly 6 bend excepted) is encouraging. Also, the calculated and observed spreading rates (Figs 7 and 4) are generally similar. The main discrepancy occurs between the *ca.* 14 mm yr^{-1} between anomalies 8 and 13 in Fig. 4 and the *ca.* 10 mm yr^{-1} of Fig. 7. This may result from the disruption of the relevant part of profiles D, E and F in Fig. 4: the apparent spreading rate on profile B is smaller. Thus, in summary, we can be confident that the change in spreading direction at or about anomaly 6 time is real.

The second prominent feature of Fig. 7 is the extensive region of ocean floor which was not formed at any of the ridge crest sections of the SAAR which survive today. These areas (shaded in Fig. 7) unfortunately do not contain any of the confidently-identified magnetic anomaly sequences shown in Fig. 3. Their origin becomes clear, however, when it is realised that the long-offset Bullard (and South Sandwich) fracture zones could not have existed with the direction of spreading as it was before 20 Ma. This is illustrated by the reconstruction to 20 Ma (South America fixed) which forms Fig. 8. Within the shaded zone are drawn additional flow lines (dashed) extending back to 50 Ma, and the lineations extracted from SEASAT gravity data in Fig. 5. The dashed lines originate at points on the present Bullard fracture zone trace. Their general gross parallelism

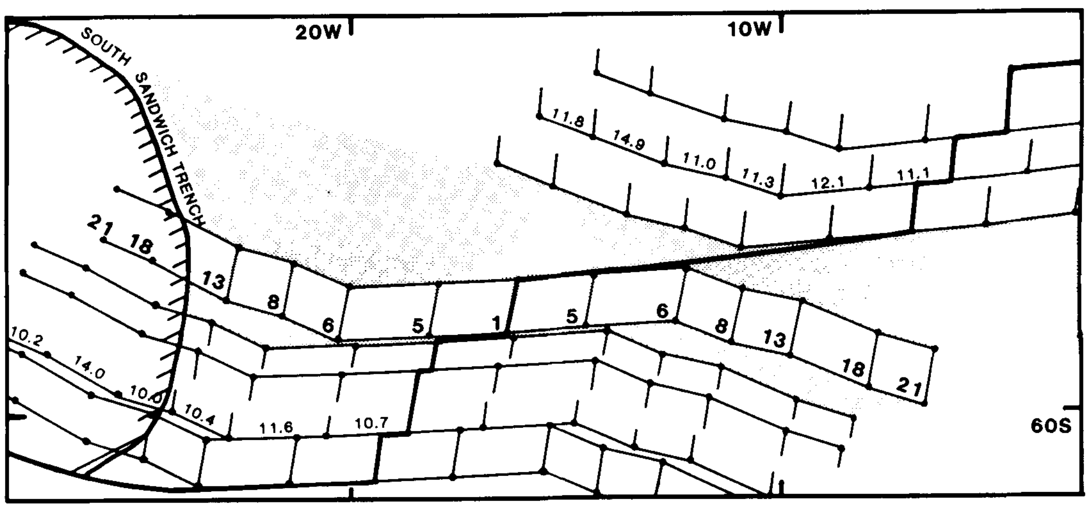

Figure 7. Synthetic small-offset fracture zone traces, extending from present-day ridge crest–transform intersections, and generated using SAM–ANT rotations from Table 1. Magnetic anomalies along one trace are numbered, and calculated half spreading rates (mm/yr) noted along two others. Shaded areas were *not* produced at any spreading ridge segments now extant.

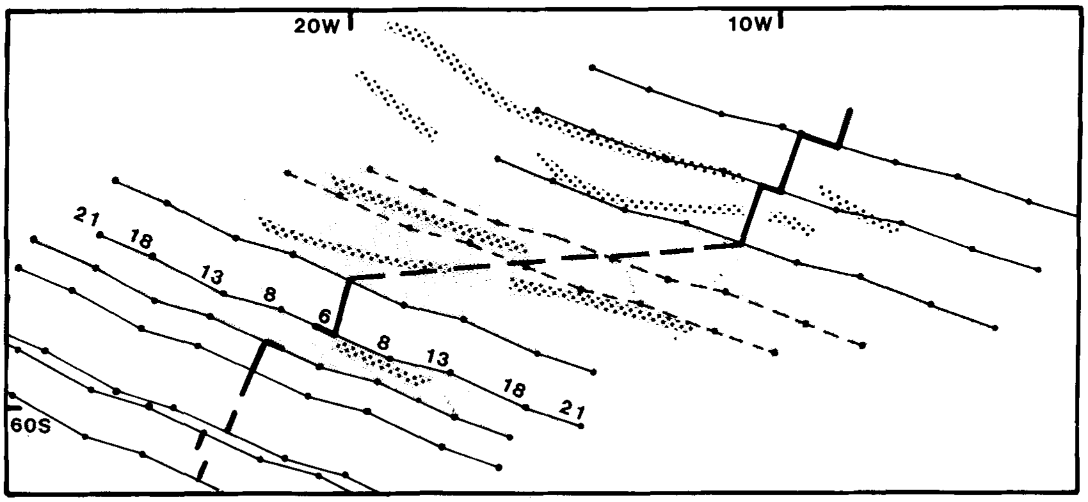

Figure 8. Synthetic fracture zones from Fig. 7, displayed on a 20 Myr (anomaly 6) reconstruction. Large shaded areas, now coincident, were produced at ridge crest sections rendered inactive by formation of Bullard fracture zone (shown dashed, along with additional synthetic fracture zone traces centred on it). Dotted stripes are lineations transferred from SEASAT interpretation in Fig. 5.

with the SEASAT data confirms the three-plate calculations, and suggests that the Bullard fracture zone cut through not too far away from the existing ridge crest sections. It is in this region, where the oceanic lithosphere was youngest and thinnest, that such a rupture is most likely to have taken place.

We have considered possible explanations for the change in spreading direction, whether a simple, local or remote change in the balance of forces on the plates can be held responsible, and the consequences for our understanding of plate motions in general. Firstly, since we have been working with the South American, African and Antarctic plates, it may be useful to see what changes in their relative motion occurred at the same time. Table 1 shows that changes in the poles of South American–African and African–Antarctic motion around 20 Ma were small. At the nearest parts of the South American–African plate boundary to the SAAR, there was a small (5 per cent) reduction in spreading rate but no change in direction. At the African–Antarctic boundary, nearby, there was a 30 per cent reduction in spreading rate (also small, since AFR–ANT motion is slow), but again no direction change. In both cases, spreading directions are constrained by long-offset transform faults, so the effect of the SAAR change may have been to make the forces on those transforms more transpressional, increasing frictional drag and thus opposing the ridge push force. At the SAAR, no observable increase in spreading rate accompanied the change in direction.

The direction change coincided with another local event at 20 Ma. This was a collision of a more westerly section of the SAAR than now exists, with an ancestor of the South Sandwich trench, east of the South Orkney micro-continent (Barker *et al.* 1984). In that this was an 'active' collision initially, until any back-arc extension in Jane Basin or Powell Basin stopped, it may have given an eastward push to the Antarctic plate, to initiate the change. Also, the collision greatly reduced the length of the SAAR, possibly making the rupture of the remaining length easier. However, no sharp, long-term change in the balance of forces on the major plates appears to have resulted from the collision, and it is difficult to see how it could have been the major cause of a stable change of direction. It may be more useful to regard this change as merely the latest of a series which have progressively rotated the direction of South American–Antarctic motion over the past 20 Myr.

It is beyond the scope of this paper to compile a model of the forces acting on the three major plates, after the manner of Wortel & Cloetingh (1981, 1983) for example, to understand the link between these forces and the plate motion change. Not that it would be possible to limit such a study to the boundaries of the South American, African and Antarctic plates: considerable shear stress could be transmitted across many of the external boundaries of these plates, so that the problem is essentially global. However, two comments are perhaps worthwhile.

(1) The importance of long transform faults in controlling the directions of plate motion has perhaps been underestimated. Considerable compressive forces may commonly occur at long transforms, and many plates may not be moving in directions related to the forces on them in the way assumed in studies such as that of Solomon, Sleep & Richardson (1975).

(2) It follows, since compressive stress can build up along transforms, that when a change in motion does occur, as at the SAAR 20 Myr ago, the 'cause', in the sense of a major change in the balance of forces on the plates, may have taken place several million years previously. The change in motion would have been delayed until a threshold stress had built up, or until a reduction in the strength of the relevant plate boundary, as suggested here, had occurred.

CONCLUSIONS

The magnetic and bathymetric data from the region east of the South Sandwich trench, are now sufficient in number and quality to provide reasonable estimates of spreading rates and directions on the SAM–ANT plate boundary, over the past 50 Myr.

(1) South American–Antarctic plate motion over this period has been slow, with half spreading rates along the South American Antarctic Ridge of between 9 and 15 mm yr^{-1}. The direction of spreading, now approximately E–W, was close to 120°–300° before about 20 Ma.

(2) These data provide local constraints on a calculation of SAM–AFR–ANT motion, using in addition existing data from the South Atlantic and SW Indian Ocean. Poles and rates of rotation have been computed for 6 stages (anomalies 5, 6, 8, 13, 18 and 21) within the past 50 Myr.

(3) Synthetic fracture zones constructed using these calculated poles and rates are compatible with the observed data and with SEASAT gravity lineations. They appear to show that the change in spreading direction at 20 Ma was reasonably abrupt, although the quality of existing data does not allow an estimate of how long the change actually took. The long-offset Bullard and South Sandwich fracture zones were created at the time of the change, probably by the rupture of oceanic lithosphere near to existing spreading ridges, where it would have been weakest. The effect of the change was to reduce the ridge crest length along the plate boundary, while increasing the fracture zone length.

(4) The direction change coincides with a ridge crest–trench collision at Jane Bank east of the South Orkney Is. This reduced the length of the simple SAM–ANT boundary and temporarily 'pushed' the Antarctic plate eastward, so may have both enabled and triggered the change. However the collision did *not* result in a large, sharp and permanent change in the balance of forces on the plates, sufficient to maintain the new direction.

(5) At the time of the SAM–ANT direction change, the effects on SAM–AFR and AFR–ANT motion were minor: the rotation poles did not move far, and there was only a small reduction in spreading rate. It is suggested that SAM–AFR and (particularly) AFR–ANT motion is constrained by the existence of long-offset fracture zones, and that the *reduction* in spreading rate observed at each boundary means that transpressive forces across these fracture zones increased as a result of the change.

(6) It seems inescapable that plates do not necessarily respond instantaneously to significant changes in the balance of forces acting upon them, but rather have to await the opportunity provided by other changes (as here perhaps, a reduction in length of lithosphere to be ruptured). Thus 'causes' of major changes in plate motion may long precede the changes themselves and computations of the balance of forces on the plates which neglect transpression may be in error. In this particular case, the change of direction may be better seen as only one more stage in the gradual rotation of the direction of SAM–ANT motion.

If the Bullard and South Sandwich fracture zones did form abruptly, by the rupture of young, thin lithosphere near the ridge crest, then the region provides the opportunity to examine another little-known mode of formation and modification of ocean floor.

ACKNOWLEDGMENTS

We are grateful to John Sclater and Chris Scotese at UTA and to Don Griffiths at Birmingham for facilities and useful discussion during the long gestation of this paper, and to Steve Cande for making data available prior to publication. The work was supported in part by research grants BAS/F60/E1/07 and DPP84-05968. Contribution No. 746 of the Institute for Geophysics, University of Texas at Austin.

REFERENCES

Barker, P. F., 1970. Plate tectonics of the Scotia Sea region, *Nature,* **228,** 1293–1296.

Barker, P. F., 1979. The history of ridge-crest offset at the Falkland–Agulhas fracture zone from a small-circle geophysical profile, *Geophys. J. R. astr. Soc.,* **59,** 131–145.

Barker, P. F. & Burrell, J., 1977. The opening of Drake Passage, *Mar. Geol.,* **25,** 15–34.

Barker, P. F. & Hill, I. A., 1981. Back-arc extension in the Scotia Sea, *Phil. Trans. R. Soc. A,* **300,** 249–262.

Barker, P. F. & Jahn, R. A., 1980. A marine geophysical reconnaissance of the Weddell Sea, *Geophys. J. R. astr. Soc.,* **63,** 271–283.

Barker, P. F., Barber, P. L. & King, E. C., 1984. An early Miocene ridge crest-trench collision on the South Scotia Ridge near 36W, *Tectonophys.,* **102,** 315–332.

Bergh, H. W. & Norton, I. A., 1976. Prince Edward fracture zone and the evolution of the Mozambique Basin, *J. geophys. Res.,* **81,** 5221–5239.

Cande, S. C. & Leslie, R. B., 1986. Late Cenozoic tectonics of the southern Chile trench, *J. geophys. Res.,* **91,** 471–496.

Cande, S. C., Herron, E. M. & Hall, B. R., 1982. The Early Cenozoic tectonic history of the southeast Pacific, *Earth planet. Sci. Lett.,* **57,** 63–74.

Chase, C. G., 1978. Plate kinematics: the Americas, East Africa and the rest of the world, *Earth planet. Sci. Lett.* **37,** 355–368.

Farmer, R. A., Fujita, K. & Stein, S., 1982. Seismicity and tectonics of the Scotia Sea area, *Eos, Trans. Am. geophys. Un.,* **63,** 440.

Fisher, R. L. & Sclater, J. G., 1983. Tectonic evolution of the Southwest Indian Ocean since the mid-Cretaceous: plate motions and stability of the pole of Antarctica–Africa for at least 80 Ma, *Geophys. J. R. astr. Soc.,* **73,** 553–576.

Forsyth, D. W., 1975. Fault plane solutions and tectonics of the South Atlantic and Scotia Sea, *J. geophys. Res.,* **80,** 1429–1443.

Goslin, J., Recq, M. & Schlich, R., 1981. Structure profonde du plateau de Madascar: relations avec le plateau de Crozet, *Tectonophys.,* **101,** 75–97.

Haxby, W. F., 1985. *Gravity field of the world's oceans,* U.S. Navy, Office of Naval Research and Lamont–Doherty Geological Observatory Chart.

Hellinger, S. J., 1981. The uncertainties of finite rotations in plate tectonics, *J. geophys. Res.,* **86,** 9312–9318.

Herron, E. M., Cande, S. C. & Hall, B. R., 1981. An active spreading centre collides with a subduction zone: a geophysical survey of the Chile margin triple junction, *Mem. geol. Soc. Am.,* **154,** 683–701.

I.A.G.A., 1981. International geomagnetic reference fields: DGRF 1965, DGRF 1970, DGRF 1975, and IGRF 1980, *Eos, Trans. Am. geophys. Un.,* **62,** 1169.

Isacks, B. L. & Molnar, P., 1971. Distribution of stresses in the descending lithosphere from a global survey of focal mechanism solutions of mantle earthquakes, *Rev. geophys. Space Phys.,* **9,** 103–174.

LaBrecque, J. L. & Barker, P. F., 1981. The age of the Weddell Basin, *Nature,* **290,** 489–492.

LaBrecque, J. L. & Hayes, D. E., 1979. Seafloor spreading history of the Agulhas basin, *Earth planet. Sci. Lett.*, **45,** 411–428.

LaBrecque, J. L., Kent, D. V. & Cande, S. C., 1977. Revised magnetic polarity time scale for late Cretaceous and Cenozoic time, *Geology,* **5,** 330–335.

Ladd, J. W., 1974. South Atlantic sea-floor spreading and Caribbean tectonics, *PhD thesis,* Columbia University, New York.

Lawver, L. A. & Dick, H. J. B., 1983. The America–Antarctic ridge, *J. geophys. Res.*, **88,** 8193–8202.

Lawver, L. A., Sclater, J. G. & Meinke, L., 1985. Mesozoic and Cenozoic reconstructions of the South Atlantic. *Tectonophys.*, **114,** 233–254.

Menard, H. W., 1978. Fragmentation of the Farallon plate by pivoting subduction, *J. Geol.*, **86,** 99–110.

Minster, J. B. & Jordan, T. H., 1978. Present-day plate motions, *J. geophys. Res.*, **83,** 5331–5354.

Norton, I. O. & Sclater, J. G., 1979. A model for the evolution of the Indian Ocean and the break-up of Gondwanaland, *J. geophys. Res.*, **84,** 6803–6830.

Parsons, B. L. & Sclater, J. G., 1977. An analysis of the variation of ocean floor bathymetry and heat flow with age, *J. geophys. Res.*, **82,** 803–827.

Patriat, P. L., 1983. Reconstitution de l'evolution du systeme de dorsales de l'Ocean Indien, par les methodes de la cinematiques des plaques, *These Doctorat d'Etat,* Universite Pierre et Marie Curie, Paris.

Rabinowitz, P. D. & LaBrecque, J. L., 1979. The Mesozoic South Atlantic ocean and evolution of its continental margins, *J. geophys. Res.*, **84,** 5973–6002.

Schlich, R., 1983. The Indian Ocean: aseismic ridges, spreading centers and oceanic basins, in *The Ocean Basins and Margins, vol.* 6, *The Indian Ocean,* eds Nairn, A. E. M. & Stehli, F. G., Plenum Press, New York.

Scotese, C. R., Gahagan, L. & Larson, R., 1988. Plate tectonic reconstructions of the Mesozoic and Cenozoic ocean basins, *Tectonophys.*, in press.

Sclater, J. G., Bowin, C., Hey, R., Hoskins, J., Peirce, J., Phillips, J. & Tapscott, C., 1976. The Bouvet triple junction, *J. geophys. Res.*, **81,** 1857–1869.

Solomon, S. C., Sleep, N. H. & Richardson, R. H., 1975. On the forces driving plate tectonics: inferences from absolute plate velocities and intraplate stress, *Geophys. J. R. astr. Soc.*, **42,** 769–801.

Tapscott, C., 1979. Evolution of the Indian Ocean triple junction and the finite rotation problem, *PhD thesis,* Massachusetts Institute of Technology/Woods Hole Oceanographic Institution, WHOI-80-37.

Tectonic Map of the Scotia Arc, 1:3000000, BAS (Misc) 3, Cambridge, British Antarctic Survey, 1985.

Wortel, R. & Cloetingh, S., 1981. On the origin of the Cocos–Nazca spreading center, *Geology,* **9,** 425–430.

Wortel, R. & Cloetingh, S., 1983. A mechanism for fragmentation of oceanic plates, in *Studies in Continental Margin Geology,* eds Watkins, J. S. & Drake, C. L., *Mem. Am. Ass. Petrol. Geol.*, **34,** 793–801.